

10 Tropical zonal and meridional circulations

More reading:

1. Rodwell MJ, Hoskins BJ (2001) Subtropical Anticyclones and Summer Monsoons. *J Clim*, **14**, 3192–3211
2. Chao WC, Chen B (2001) The origin of Monsoons. *J Atmos Sci*, **58**, 3497–350
3. Kucharski, F, Bracco, A, Barimalala, R, Yoo, J-H (2011) Contribution of the east–west thermal heating contrast to the South Asian Monsoon and consequences for its variability, *Clim Dyn*, **37**, 721–735, DOI 10.1007/s00382-010-0858-3

Let’s have a look at the global June-to-September rainfall distribution in Fig. 46. We can clearly identify the Intertropical Convergence Zone (ITCZ), identified by the rainfall maximum north of the equator that can reach 30°N in some land region. We also see that this strip of large rainfall is not zonally homogeneous, but is stronger in some locations than in others. Some of the features may be explained by the distributions of sea surface temperatures (SSTs) in Fig. 47. Note that the rainfall is the column integrated $-L_{lv} \frac{dm_v}{dt}$ and therefore related to the column integrated diabatic heating due to condensation according to Eqs. 171 and 46.

The western Pacific rainfall maximum is related to high SSTs in that region, as we have already discussed several times. Also, the land-sea contrast are likely important due to different heat capacities. As we have already discussed regarding the ENSO phenomenon, the distribution of SSTs, rainfall and atmospheric circulations in the tropical Pacific provide positive feedbacks between them, so that its difficult to say what is cause and what is effect (chicken-egg problem). The mean zonal circulation in the tropical regions is called *Walker circulation* (see also Fig. 20). Note that this circulation is not a strict closed circulation cell as we could derive for the zonal mean circulation (Hadley Cell). A good measure of this zonal tropical circulation is the upper-level *velocity potential*, χ , for which we have the relation to the divergent wind

$$\mathbf{v}_\chi = \nabla \chi \quad (242)$$

The distribution of the 200 hpa velocity potential χ is shown in Fig. 48a (which height is this, approximatively). According to the definition 242, a minimum means divergent wind. The centre of upper-level divergence (rising motion, why?) is in the western Pacific region, and the centers of upper-level convergence (sinking motion, why?) are located in the eastern Pacific (that is the classical Walker circulation) and in the tropical South Atlantic region.

Fig. 48 b) shows the *streamfunction*, ψ , which is related to the rotational flow in the following way (see, e.g. Eq. 16)

$$\mathbf{v}_\psi = \mathbf{k} \times \nabla \psi \quad . \quad (243)$$

It is clear that there is a systematic relationship between upper-level velocity potential and upper-level streamfunction, they are in 'quadrature', that is the extreme values of one lie in the gradient regions of the other. Can we propose an explanation for this behaviour? The solution is an approximate version of the vorticity equation 67 for the tropics

$$\frac{d_g \xi_g}{dt} = -f_0 \left(\frac{\partial u_a}{\partial x} + \frac{\partial v_a}{\partial y} \right) - \beta v_g \quad . \quad (244)$$

It turns out that in the tropical regions relative vorticity changes and advections are relatively small, mainly because of approximate geostrophy and small pressure gradients. We may estimate it to be one order of magnitude smaller than in the extratropics. Therefore, the left hand side is Eq. 244 may be set to zero. This leaves us with the approximation

$$\beta v_\psi = -f_0 \left(\frac{\partial u_\chi}{\partial x} + \frac{\partial v_\chi}{\partial y} \right) \quad , \quad (245)$$

where we have used that the geostrophic wind is the rotational wind defined in Eq. 243 (note that according to the quasigeostrophic vorticity definition 66, $\psi = \Phi/f$ is the streamfunction as long as we are not too close to the equator), and the ageostrophic wind is the divergent wind defined in Eq. 242. Eq. 245 is called *Sverdrup balance*. If we take a divergence field as given (e.g. the field that corresponds to Fig. 48a; we can imagine it has been caused by the dominance of the west Pacific heating), then according to the Sverdrup balance, this will cause rotational winds. An upper level divergence maximum will lead to southward rotational motion in the northern hemisphere, an upper-level convergence maximum will lead to northward rotational motion. This is consistent with the streamfunction distribution in Fig. 48b, and explains why velocity potential and streamfunction are in quadrature (exercise!). Note that the interpretation of the Asian monsoon high to be partially forced by Sverdrup balance from the heating differences between the western Pacific and the Atlantic Ocean is a relatively new one. The conventional point of view is that the Asian monsoon high (*Tibetan high*) is forced exclusively by the land sea contrast between the Asian land mass (including importance of Himalayas) and the Indian Ocean. We also note that all the structures that we have considered for upper levels should be reversed for low levels, thus a part of the low-level monsoon trough can be attributed to the western Pacific/Atlantic heating differences. Keep in mind that secondary vertical motions can be induced then by surface friction, because the streamfunction centres that we can derive are fields with vorticity, which according to equation 221 induces vertical motion (see section 8). Positive (negative) vertical motion, in turn, leads to increased (decreased) rainfall (why?). These effects have been analysed with idealized numerical experiments in the paper cited in the beginning of the section (see also Figs. 49, 50, 51).

Exercises

1. Let the velocity potential distribution in zonal direction at latitude 30°N be

$$\chi = A\cos(\lambda) ,$$

where λ is longitude. Calculate using the Sverdrup balance 245 to derive the zonal distribution of the streamfunction at the same latitude.

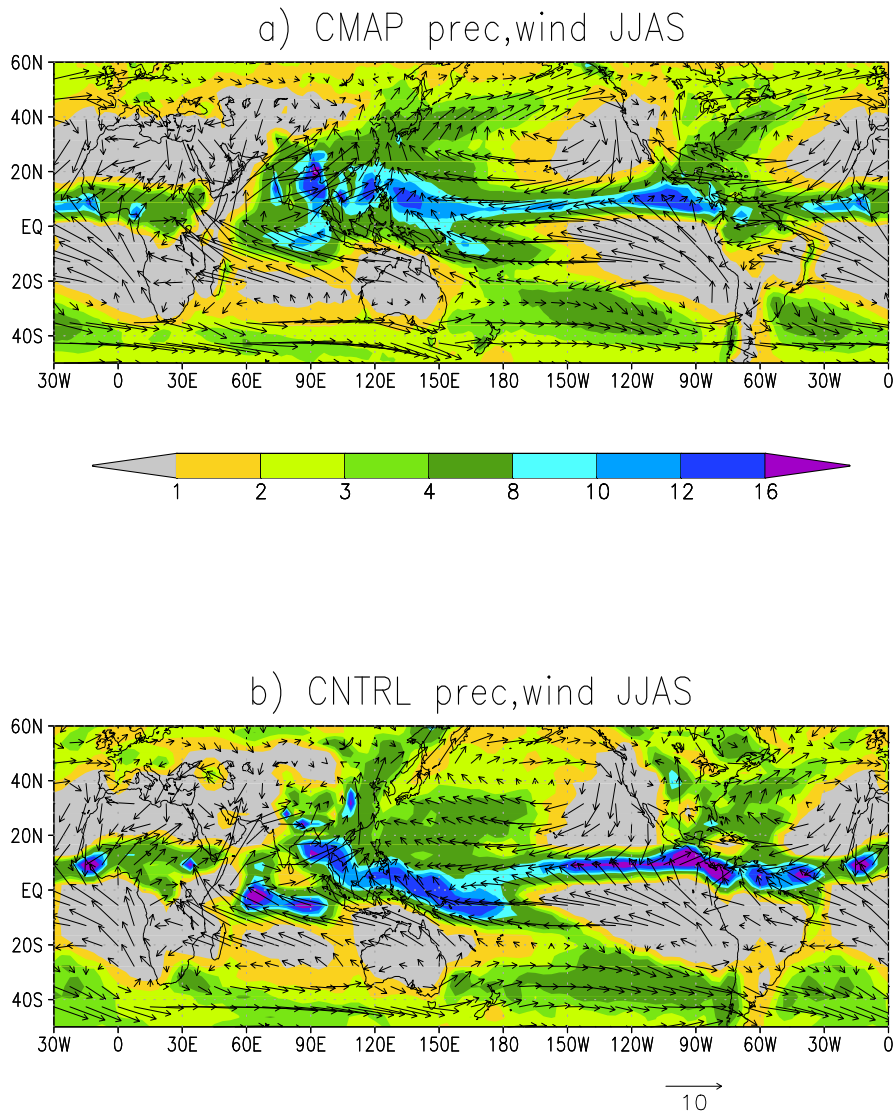


Figure 46: Mean JJAS rainfall and surface winds a) from observations (CMAP,NCEP-NCAR re-analysis), b) from the ICTPAGCM. Units are mm/day for rainfall and m/s for wind.

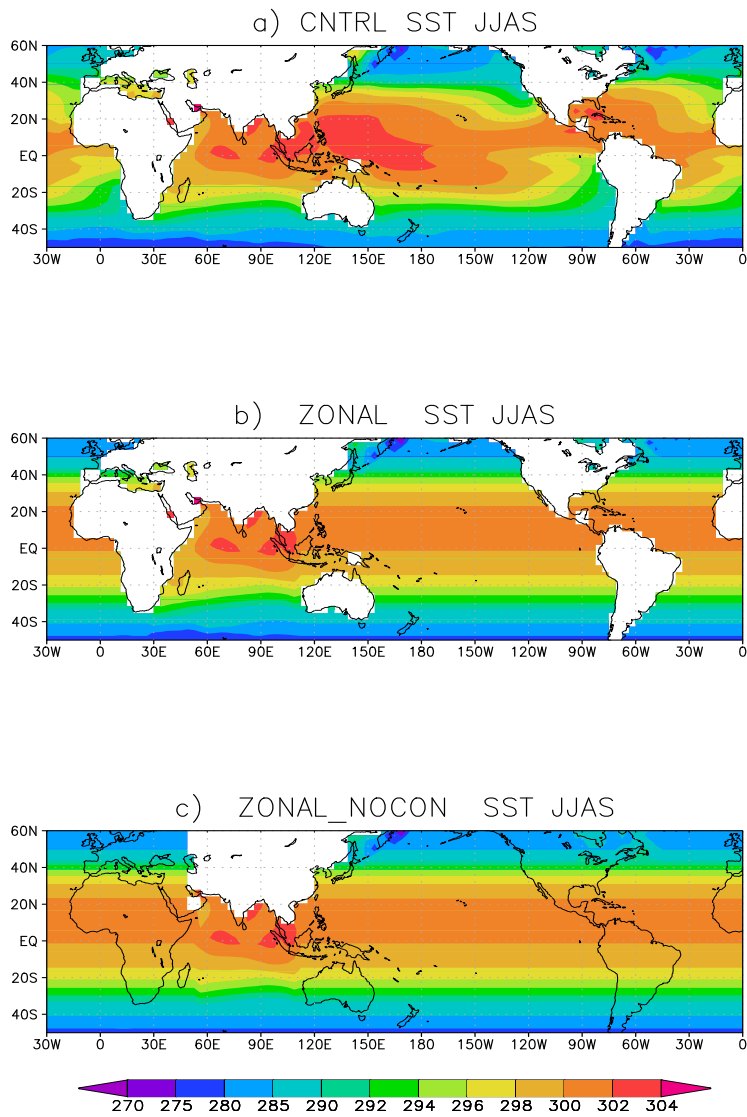


Figure 47: Mean JJAS sea surface temperature distribution a) observed, b) and c) idealized distribution for numerical experimentation.

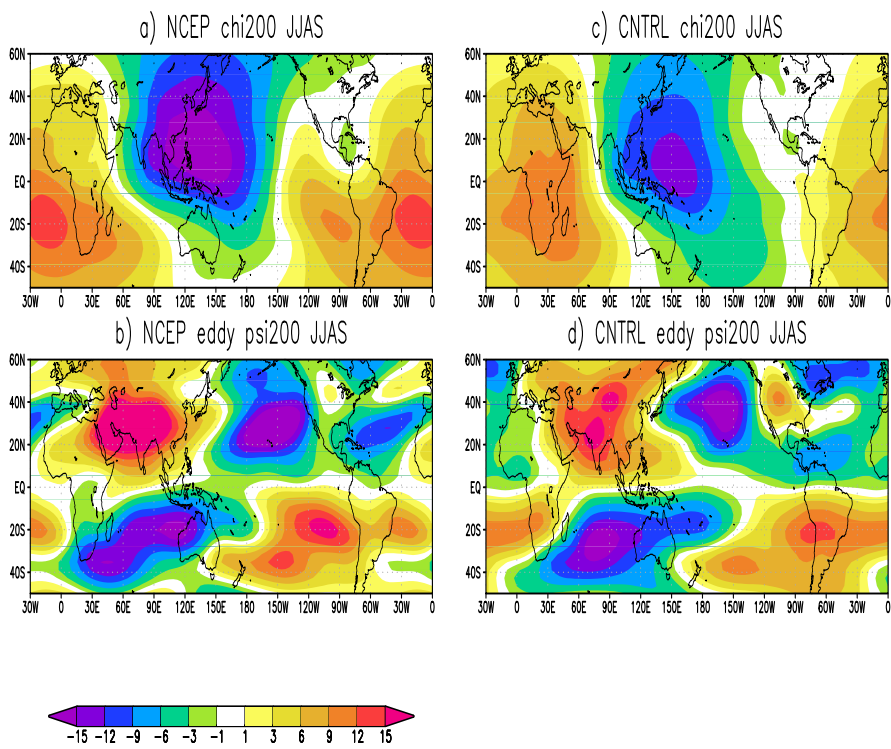


Figure 48: Mean JJAS distributions at 200 hPa of a) observed velocity potential χ , c) modeled observed velocity potential χ , b) observed streamfunction ψ , d) modeled streamfunction ψ . Units are $10^6 \text{ m}^2 \text{ s}^{-2}$.

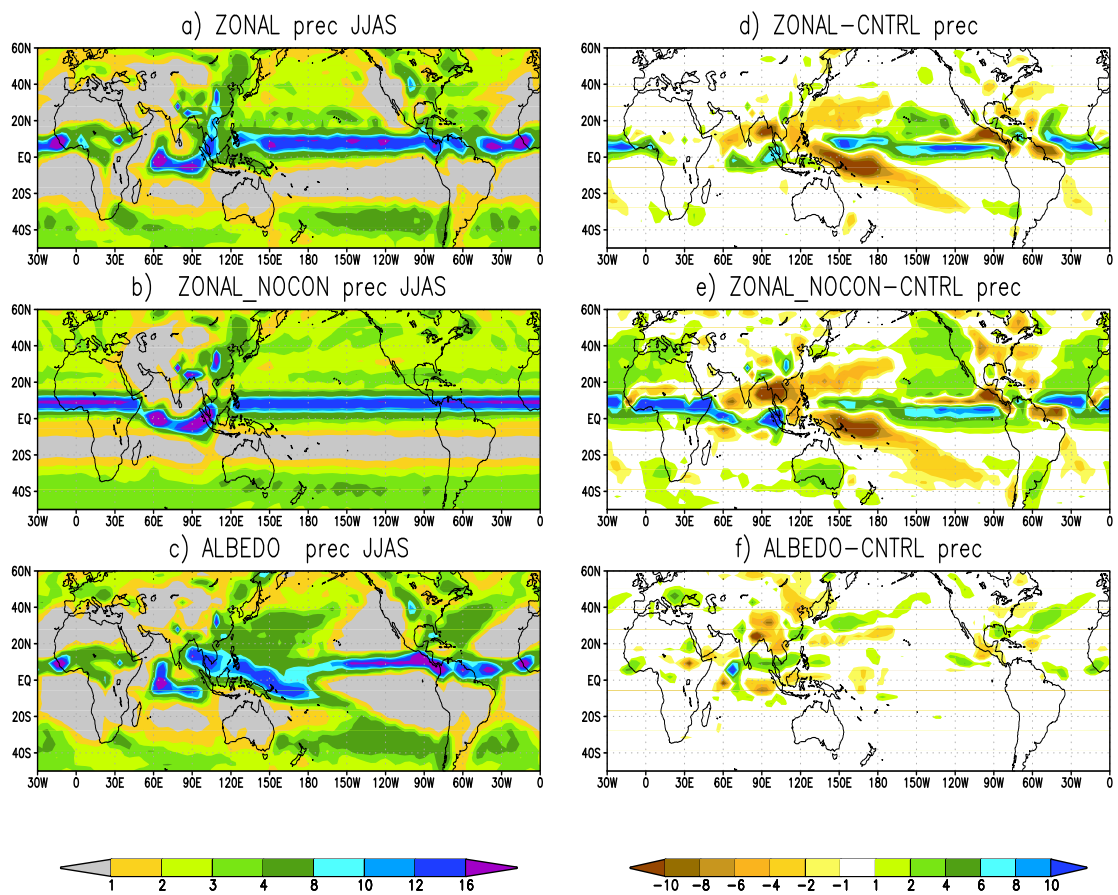


Figure 49: Response in rainfall to zonal (a, d)) and zonal with removed African and American continents (b, e). Units are mm/day.

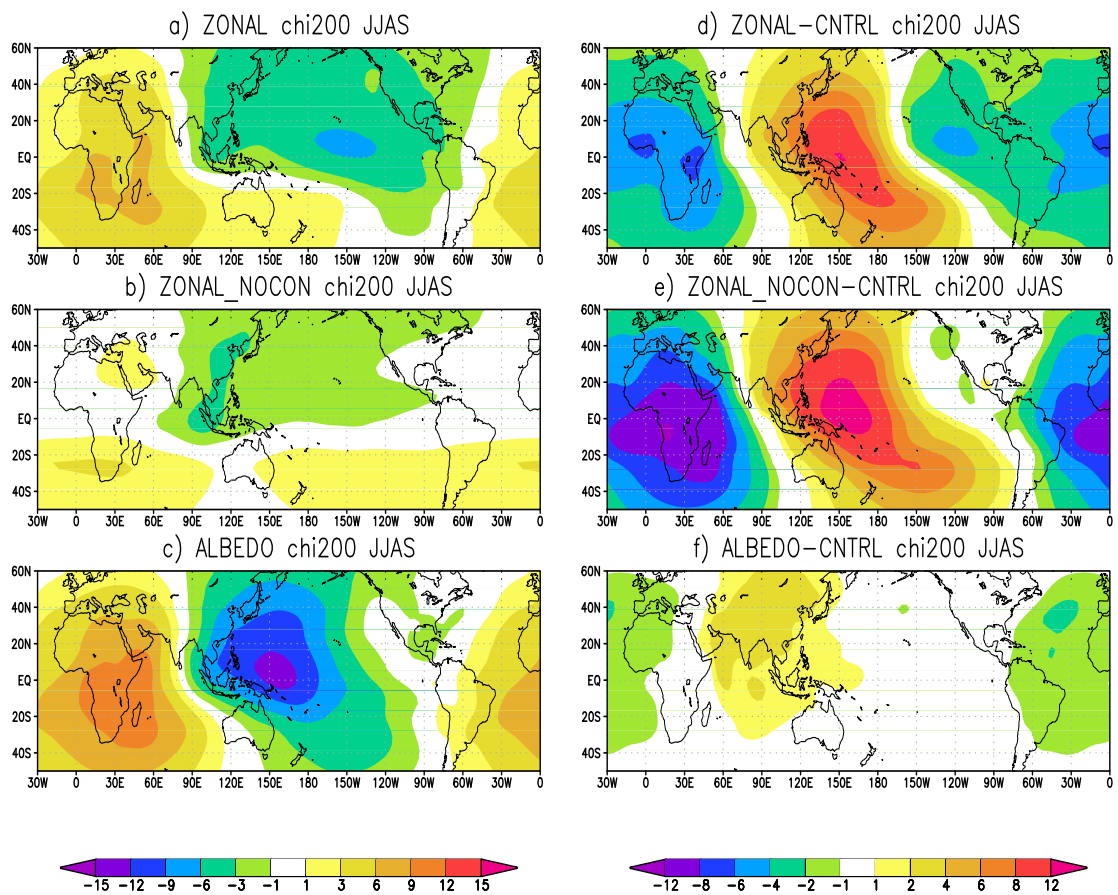


Figure 50: Response in velocity potential χ to zonal (a, d)) and zonal with removed African and American continents (b, e). Units are $10^6 \text{ m}^2 \text{ s}^{-2}$.

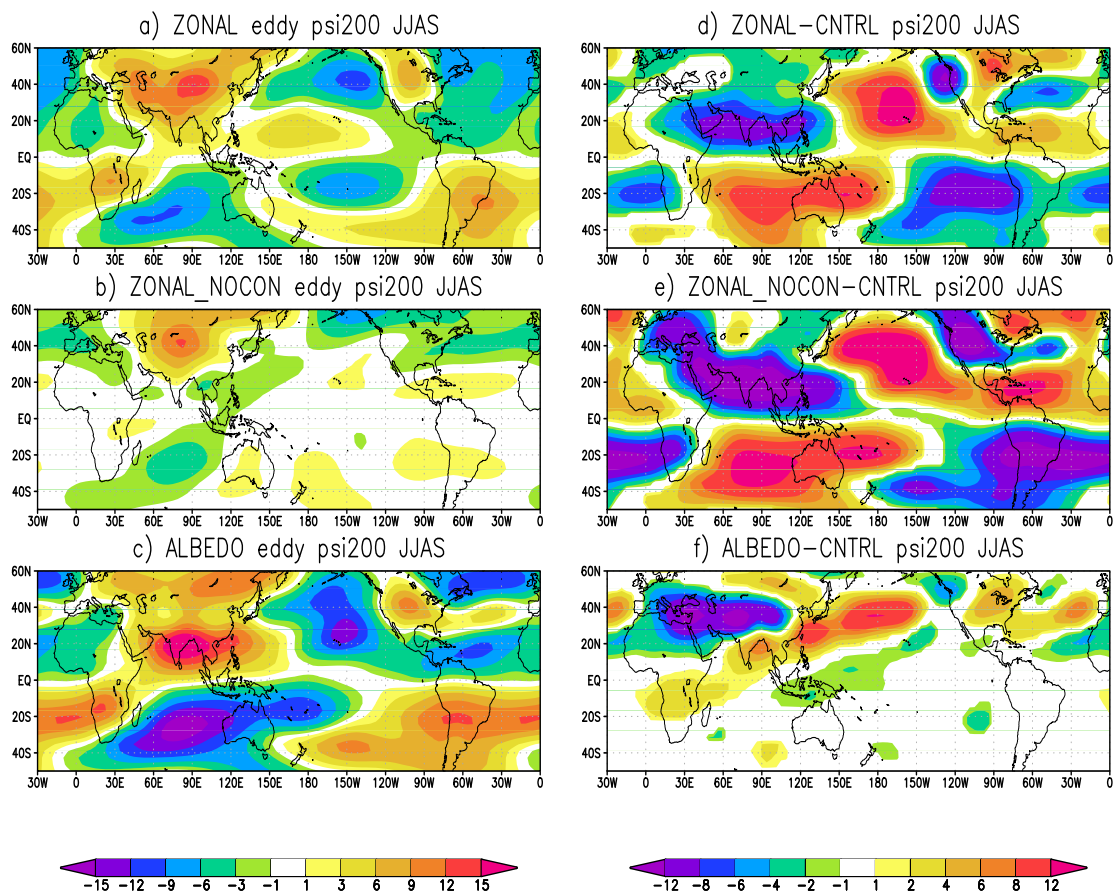


Figure 51: Response in eddy streamfunction ψ to zonal (a, d)) and zonal with removed African and American continents (b, e). Units are $10^6 \text{ m}^2 \text{ s}^{-2}$.